Akt1 Is Required for Physiological Cardiac Growth

Brian DeBosch, BS; Iya Treskov, BS; Traian S. Lupu, DVM; Carla Weinheimer, MS; Attila Kovacs, MD; Michael Courtois, MA; Anthony J. Muslin, MD

Background—Postnatal growth of the heart chiefly involves nonproliferative cardiomyocyte enlargement. Cardiac hypertrophy exists in a "physiological" form that is an adaptive response to long-term exercise training and as a "pathological" form that often is a maladaptive response to provocative stimuli such as hypertension and aortic valvular stenosis. A signaling cascade that includes the protein kinase Akt regulates the growth and survival of many cell types, but the precise role of Akt1 in either form of cardiac hypertrophy is unknown.

Methods and Results—To evaluate the role of Akt1 in physiological cardiac growth, $akt1^{-/-}$ adult murine cardiac myocytes (AMCMs) were treated with IGF-1, and $akt1^{-/-}$ mice were subjected to exercise training. $akt1^{-/-}$ AMCMs were resistant to insulin-like growth factor-1–stimulated protein synthesis. The $akt1^{-/-}$ mice were found to be resistant to swimming training–induced cardiac hypertrophy. To evaluate the role of Akt in pathological cardiac growth, $akt1^{-/-}$ AMCMs were treated with endothelin-1, and $akt1^{-/-}$ mice were subjected to pressure overload by transverse aortic constriction. Surprisingly, $akt1^{-/-}$ AMCMs were sensitized to endothelin-1–induced protein synthesis, and $akt1^{-/-}$ mice developed an exacerbated form of cardiac hypertrophy in response to transverse aortic constriction.

Conclusions—These results establish Akt1 as a pivotal regulatory switch that promotes physiological cardiac hypertrophy while antagonizing pathological hypertrophy. **(*Circulation*. 2006;113:2097-2104.)**

Key Words: heart failure ■ hypertrophy ■ signal transduction

Postnatal mammalian cardiomyocytes respond to mechanical stress, growth factors, hormones, and metabolic and sarcomeric abnormalities by enlarging. Nearly all of these cells, however, are unable to proliferate.[1] The clinical consequences of cardiac hypertrophy include the development of cardiac arrhythmia, diastolic dysfunction, and congestive heart failure.[2,3] The cardiac hypertrophic response, however, is not universally associated with a poor prognosis. Indeed, cardiac hypertrophy in well-trained athletes does not progress to congestive heart failure.[4,5]

Editorial p 2032
Clinical Perspective p 2104

The phosphatidylinositol-3-kinase (PI3K)-Akt pathway has been investigated as a participant in the cardiac hypertrophic program. Although the first genetic evidence that this pathway is critical for cellular growth was derived from studies in *Drosophila melanogaster*,[6] this idea was recently confirmed both in vertebrate tissue cultures and in mice. PI3K or activated Akt overexpression in various mouse tissues leads to organ enlargement, and in all cases, increased cell size is a major contributor to the phenotype.

There are 3 members of the Akt family: Akt1, Akt2, and Akt3.[7,8] Each member has a highly conserved protein kinase domain and a pleckstrin homology domain, which is required for Akt activation. Activated Akt proteins phosphorylate a variety of intracellular substrates that regulate growth, metabolism, and survival. Akt phosphorylates and inhibits the product of the *TSC2* gene, tuberous sclerosis 2 (TSC2), which itself inhibits the mammalian target of rapamycin.[9,10] Recent work has emphasized the control of protein synthesis by the mammalian target of rapamycin, an important effector that promotes growth.[11] The Foxo family of fork-head transcription factors[12] and glycogen synthase kinase–3 (GSK-3)[13] also are important negative regulators of protein synthesis that are inhibited by Akt.

PI3K and Akt1 are activated in rodent heart in response to pressure overload and in cultured cardiomyocytes in response to hypertrophic ligands.[14] Treatment of cultured cardiomyocytes with PI3K inhibitors blocked ligand-induced hypertrophy.[15] Cardiac-specific overexpression of activated PI3K(p110α) in transgenic mice resulted in baseline cardiac hypertrophy without fibrosis.[16] Conversely, cardiac-specific expression of a dominant-negative p110α mutant resulted in reduced heart size and weight associated with normal cardiac function.[17] Cardiac-specific overexpression of activated mutant (dd)Akt1 resulted in massive cardiac hypertrophy and fibrosis associated with normal contractile function.[18]

Received October 13, 2005; revision received February 13, 2006; accepted February 17, 2006.

From the Center for Cardiovascular Research, Department of Medicine (B.D., I.T., T.S.L., C.W., A.K., M.C., A.J.M.), and Department of Cell Biology and Physiology (B.D., I.T., T.S.L., A.J.M.), Washington University School of Medicine, St Louis, Mo.

The online-only Data Supplement can be found at http://circ.ahajournals.org/cgi/content/full/CIRCULATIONAHA.105.595231/DC1.

Correspondence to Anthony J. Muslin, Center for Cardiovascular Research, Box 8086, Washington University School of Medicine, 660 S Euclid Ave, St. Louis, MO 63110. E-mail amuslin@imgate.wustl.edu

Circulation **is available at http://www.circulationaha.org** **DOI: 10.1161/CIRCULATIONAHA.105.595231**

Cardiac-specific membrane-anchored Akt1 (myr-Akt1) overexpression models exhibited a comparable baseline cardiac growth phenotype.[19] Although some investigators have argued for Akt as a major regulator of physiological hypertrophy, some experiments are consistent with Akt also promoting pathological hypertrophy.[18]

Akt1 and Akt2 appear to have distinct biological functions. akt2$^{-/-}$ mice exhibit defective insulin-stimulated glucose uptake in muscle and fat,[20] implicating Akt2 in glucose homeostasis. In contrast, akt1$^{-/-}$ mice exhibit normal glucose homeostasis, but their body and organ sizes are proportionally 20% less than that of wild-type (WT) littermates throughout their lifespan.[21] In the present study, we analyzed the ability of Akt1-deficient mice to develop cardiac hypertrophy in response to provocative stimuli.

Methods

akt1$^{+/-}$ and akt1$^{-/-}$ Mice

Mice with targeted disruption of the akt1 gene in the C57Bl/6 genetic background were generated as previously described.[21] Mice were repeatedly backcrossed (>6 times) with WT C57Bl/6 mice obtained from the Jackson Laboratory (Bar Harbor, Me) before experimentation. Progeny were screened by tail-prep PCR. All animal procedures were approved by the Committee for Handling and Care of Laboratory Animals before experimentation. Experiments with mouse models were performed in strict accordance with the Committee for Handling and Care of Laboratory Animals protocols (Washington University approval 20030049).

Adult Murine Cardiomyocyte Cultures

Adult murine cardiomyocytes (AMCMs) were prepared according to published AFCS protocols.[22] Briefly, 8- to 12-week-old mice were killed, and their hearts were cannulated on a 16-gauge needle. Collagenase (1 mg/mL) maintained at 37°C was circulated through the coronary arterial system for ≈20 minutes. Hearts were minced, and dissolved calcium was introduced into the medium. AMCMs were then plated onto laminin-coated tissue culture vessels and serum deprived (modified Eagle's medium/Hanks' balanced salt solution containing 10 mmol/L 2,3-butanedione monoxime, 0.55 g/mL transferring, and 0.5 ng/mL selenium) before experimentation.

Swimming Exercise

Eight-week-old akt1$^{+/-}$, akt1$^{-/-}$, and WT sex- and age-matched mice were subjected to a forced swimming program for 20 days as previously reported. Mice swam twice daily; each session lasted up to 90 minutes. Constant monitoring ensured the safety of the mice and prevented them from floating or holding their breath under water. After completion of the training, the mice were subjected to transthoracic echocardiography. The mice were killed, and the hearts were dissected and weighed. Left ventricular (LV) weight, tibial length (TL), and body weight (BW) were measured so that LV/TL and LV/BW could be calculated. Because both genotypes lost weight during the swim training period, we used LV/TL as the index of comparison.

Histology

Ventricular tissue was fixed in formalin, embedded in paraffin, microtome sectioned, and stained with hematoxylin and eosin. Myocyte cross-sectional areas from randomly selected high-power fields were calculated on an Axioskop microscope (Carl Zeiss, Inc, Chester, Va) using Axiovision 4.0 software.

Transverse Aortic Constriction Procedures

Anesthetized akt1$^{-/-}$, akt1$^{+/-}$, and WT mice were subjected to pressure overload by transverse aortic constriction (TAC).[23,24] Sham-operated akt1$^{-/-}$ and akt1$^{+/-}$ mice and their WT littermates were used as controls. Seven days after surgery, mice were evaluated by echocardiography. The mice were killed, and postmortem and histological studies were performed as described above.

Echocardiography

Mice were imaged in the left lateral decubitus position on a Sequoia cardiac echocardiography machine (Acuson Co, Malvern, Pa) equipped with a 15-MHz linear transducer (15–L8). Two-dimensional parasternal long- and short-axis views were recorded, as was 2D targeted M-mode tracings throughout the anterior and posterior LV walls.

Protein Analysis

Immunoblotting was performed using standard techniques. Phospho-Akt(S473), phospho–GSK-3(S9), phospho-ERK, phospho-JNK, JNK, phospho–p70 S6K(T389), and phospho-S6(S235/236) antisera were obtained from Cell Signaling Technology (Danvers, Mass). Akt1 and ERK1/2 anti-sera were obtained from Santa Cruz Biotechnology, Inc (Santa Cruz, Calif). Blots were visualized with an ECL kit (Amersham Biosciences Inc, Piscataway, NJ). Scanned blot densitometry was performed with Scion Image densitometry software.

Leucine Incorporation Assays

AMCMs were cultured in 12-well tissue culture plates and serum deprived for 4 hours before ligand addition in the presence of 1 μCi/mL [^{3}H]-leucine (16 to 24 hours). Cultures were washed in PBS before 5% trichloroacetic acid precipitation. Acid-precipitable counts were lysed in 0.2N NaOH/0.1% SDS buffer and counted in a Beckman scintillation counter in 5 mL Ultima Gold (Packard Instruments, Meridian, Conn) liquid scintillation counting fluid.

Gene Expression Analysis

Quantitative real-time RT-PCR analysis on RNA extracted from heart lysates with Trizol reagent (Invitrogen Corp, Carlsbad, Calif) was carried out with the Taqman master mix kit (Applied Biosystems, Foster City, Calif) according to the manufacturer's specifications. The measured abundances of atrial natriuretic factor (ANF) and β-MHC mRNA were normalized to GAPDH in each sample as an internal loading control.

Statistical Analysis

Normality and equal-variance assumptions were assessed by Levene's test using the SigmaStat Statistical Analysis Package (version 3.1). Mann-Whitney rank-sum tests with Bonferroni's post hoc correction were used in comparisons for which normality or equal-variance assumptions were invalid. When indicated, data sets were compared by 2-sample, 2-tailed homoscedastic t tests with Bonferroni's post-hoc correction. In other instances, 1-way ANOVA, followed by Tukey's honestly significant difference post-hoc correction, was calculated by SigmaStat (version 3.1) or with VasarStats Statistical Software.

The authors had full access to the data and take full responsibility for its integrity. All authors have read and agree to the manuscript as written.

Results

Normal Gross Anatomic and Molecular Baseline Cardiac Characteristics in Akt1-Deficient Mice

The akt1$^{-/-}$ mice were recently generated[21] and are live born, are fertile, and have a lifespan of normal duration. Unperturbed WT and Akt-1–deficient mice were examined by transthoracic echocardiography to determine whether akt1 deletion disrupts normal cardiac anatomic dimensions or cardiac function. Each of the LV wall dimensions measured—including the diastolic LV posterior wall thickness, diastolic interventricular septum thickness, and most notably LV mass index (LVMI)—were statistically identical in WT, akt1$^{+/-}$, and akt1$^{-/-}$ mice (Table 1). The LV internal dimen-

TABLE 1. Echocardiographic Analysis of Mice at Baseline

	WT (n=20)	akt1$^{+/-}$ (n=8)	akt1$^{-/-}$ (n=5)
Heart rate, min^{-1}	684±12	706±6.87	707±7.23
LVPWd, mm	0.62±0.02	0.67±0.02	0.62±0.03
IVSd, mm	0.64±0.02	0.67±0.03	0.64±0.03
LVIDd, mm	3.36±0.07	3.59±0.06	3.34±0.10
LVMI, mg/g	2.85±0.11	3.04±0.20	3.08±0.24
LVIDs, mm	1.40±0.07	1.78±0.05*	1.44±0.03
FS, %	58.6±1.65	50.37±1.19*	56.88±1.32

n indicates the number of mice analyzed in each group; LVPWd, diastolic left ventricular posterior wall thickness; and IVSd, diastolic interventricular septal thickness. Eight- to twelve-week-old mice subjected to no intervention underwent transthoracic echocardiography. Values are mean±SE.

*P<0.05 vs WT mice.

sion at systole (LVIDs) was greater in akt1$^{+/-}$ mice compared with WT mice; therefore, the percent fractional shortening (FS) in akt1$^{+/-}$ mice was modestly lower than that in WT littermates. The normal heart rate and normal FS in akt1$^{-/-}$ mice demonstrated preserved cardiac function in unperturbed akt1$^{-/-}$ mice relative to unperturbed WT mice.

Previous work by Cho et al[21] showed that Akt2 and Akt3 expression does not increase in akt1$^{-/-}$ mouse embryonic fibroblasts cells as a compensatory mechanism. Baseline levels of individual Akt isoforms and related proteins were analyzed in AMCMs to confirm that molecular compensation does not occur in akt1$^{-/-}$ mice. Western blot analysis of WT and akt1$^{-/-}$ cardiac lysates verified the absence of Akt1 protein in akt1$^{-/-}$ mice. Importantly, no differences in baseline Akt2, ILK, and PI3Kα protein abundance (Data Supplement Figure I) were observed in akt1$^{-/-}$ mice. Akt3 abundance was below detection levels in the myocardium (not shown). Immunoblot analysis of LV lysates from WT, akt1$^{+/-}$, and akt1$^{-/-}$ mice revealed an ≈50% reduction in total Akt1 abundance in akt1$^{+/-}$ mice compared with WT mice (Data Supplement Figure II).

Insulin-Like Growth Factor-1 Signal Transduction and Protein Synthesis Is Akt1 Dependent

Swimming training of rodents increases myocardial IGF-1 gene expression,[25] and insulin-like growth factor-1 (IGF-1) treatment of AMCMs is an in vitro model of physiological hypertrophy. To test whether IGF-1 activates downstream growth-promoting signaling intermediates via Akt1, AMCMs from adult WT and akt1$^{-/-}$ mice were incubated with IGF-1 (10 nmol/L) for 0 to 10 minutes. Lysates derived from IGF-1–treated AMCMs were analyzed by phosphospecific Akt, GSK-3β, p70 S6 kinase (S6K), and S6 immunoblotting (Figure 1A). Although IGF-1 induced robust phosphorylation of each signaling intermediate in WT AMCMs, IGF-1–stimulated akt1$^{-/-}$ AMCMs exhibited attenuated IGF-1 signaling.

The requirement for Akt1 in IGF-1–stimulated cardiac Akt pathway signaling prompted us to determine whether IGF-1–stimulated cardiac growth is Akt1 dependent. Enhanced protein synthesis is a marker of cardiomyocyte hypertrophy at the cellular level. Therefore, [^{3}H]-leucine incorporation was

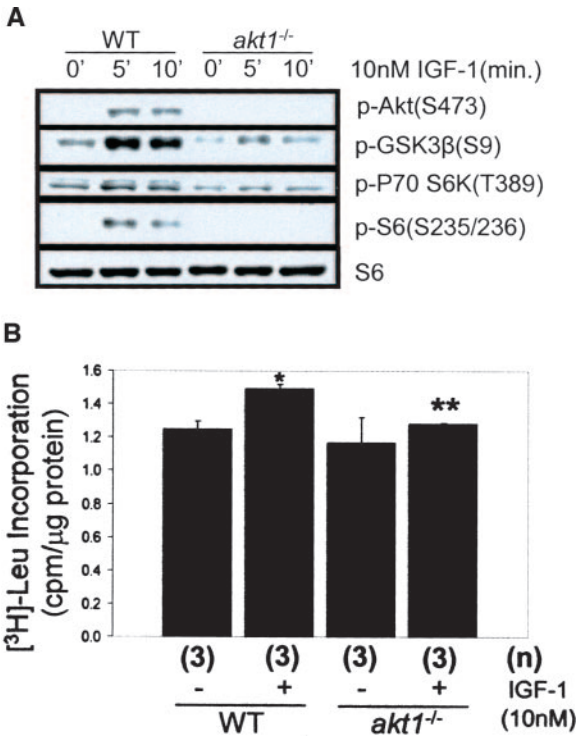

Figure 1. Akt1 is required for IGF-1–stimulated signal transduction in cultured cardiomyocytes. A, AMCMs from WT and akt1$^{-/-}$ mice were serum deprived (4 hours) and incubated with IGF-1 (10 nmol/L) for 0, 5, and 10 minutes. Lysates were analyzed by phosphospecific Akt (S473), GSK-3β(S9), p70 S6K(T389), and S6(S235/236) immunoblotting. Total S6 (bottom) was probed to control for protein loading. B, Radiolabeled leucine incorporation was measured in WT and akt1$^{-/-}$ AMCMs stimulated with vehicle or with IGF-1 (10 nmol/L) for 18 hours in the presence of [^{3}H]-leucine. Data are expressed as mean trichloroacetic acid–precipitable cpm/μg protein±SD. Sample sizes analyzed in each experiment (n) are shown in parentheses. This experiment was performed twice, and each experiment showed similar results. Shown are the mean±SD from a single, representative experiment. One-way ANOVA with Tukey's post hoc correction was performed to simultaneously compare WT unstimulated, akt1$^{-/-}$ unstimulated, WT stimulated, akt1$^{-/-}$ unstimulated, and akt1$^{-/-}$ stimulated. *P<0.05 vs WT unstimulated controls; **P<0.05 vs IGF-1–treated WT cultures.

measured in serum-deprived AMCMs stimulated with or without IGF-1 (10 nmol/L) for 18 hours (Figure 1B). WT AMCMs responded to IGF-1 by incorporating an average of 1.49±0.03 versus only 1.25±0.05 cpm/μg protein in unstimulated control cultures. akt1$^{-/-}$ AMCMs did not exhibit statistically different baseline protein synthesis (1.17±0.15 cpm/μg protein). After 18 hours of induction by IGF-1 (10 nmol/L), akt1$^{-/-}$ AMCMs incorporated markedly less [^{3}H]-leucine compared with similarly treated WT cultures (1.28±0.007 cpm/μg protein; P<0.05 vs IGF-1–induced WT cultures).

Impaired Cardiac Growth Response to Swimming Exercise in akt1$^{-/-}$ Mice

The impaired protein synthesis in akt1$^{-/-}$ cardiomyocytes after IGF-1 stimulation led us to evaluate the ability of Akt1-deficient mice to develop cardiac hypertrophy in response to involuntary swimming training. WT and Akt1-

TABLE 2. Echocardiographic Analysis of Mice After Swimming or Rest

	WT		akt1$^{-/-}$	
	Rest (n=9)	Swim (n=7)	Rest (n=5)	Swim (n=5)
Heart rate, min^{-1}	675±22	595±13*	707±7.2	671±9.6*
LVPWd, mm	0.63±0.08	0.70±0.03	0.62±0.03	0.64±0.02
IVSd, mm	0.64±0.02	0.67±0.02	0.64±0.03	0.66±0.03
LVIDd, mm	3.45±0.08	3.66±0.09	3.34±0.10	3.90±0.12*
LVMI, mg/g	3.00±0.15	3.91±0.17*	3.08±0.24	3.55±0.17
LVIDs, mm	1.48±0.12	1.65±0.09	1.44±0.03	2.02±0.16*
FS, %	57.6±2.5	55.2±1.8	56.9±1.2	48.6±2.6*

Abbreviations as in Table 1. Mice underwent transthoracic echocardiography 21 days after initiation of swimming training or rest. Values are mean±SE. To evaluate the effect of swimming training on each genotype, the following statistical comparisons were performed with Bonferroni's post hoc correction: WT rest vs WT swimming and akt1$^{-/-}$ rest versus akt1$^{-/-}$ swimming.

*P<0.05 vs resting congenic control mice.

deficient mice were trained in 90-minute sessions twice daily for 20 days, after which cardiac function was assessed by transthoracic echocardiography in trained and untrained mice (Table 2). The LVMI increased significantly in swim-trained WT mice compared with sedentary WT mice. In contrast, the LVMI did not significantly increase in swim-trained akt1$^{-/-}$ mice compared with congenic sedentary controls. Furthermore, the LV internal dimension at diastole (LVIDd) and LVIDs in akt1$^{-/-}$ mice were significantly elevated after swimming training, indicating ventricular dilatation in akt1$^{-/-}$ mice. In comparison, LVIDd and LVIDs did not increase in WT mice after swimming training. Cardiac function, as indicated by FS, was modestly but statistically lower in trained akt1$^{-/-}$ mice compared with sedentary akt1$^{-/-}$ mice. Ventricular dilatation in trained Akt1-deficient mice may represent a compensatory mechanism to maintain cardiac output in the absence of an adequate LV hypertrophic response.

Cardiac hypertrophy also was assessed by measurement of the LV/TL ratio. WT mice developed significant cardiac hypertrophy in response to swimming training compared with sex-, age-, and weight-matched littermate control animals (Figure 2A). LV/TL increased by 19.4% in WT animals after swimming training (mean LV/TL, 3.70±0.35 for WT resting mice versus 4.43±0.35 in swim-trained mice; P=0.0003; Figure 2A). However, LV/TL observed in trained akt1$^{+/-}$ and in trained akt1$^{-/-}$ mice was significantly lower than that in trained WT mice (LV/TL in trained akt1$^{+/-}$ and trained akt1$^{-/-}$ mice, 3.84±0.56 and 3.66±0.72, respectively).

A hallmark of cardiac hypertrophy is the enlargement of individual myocytes without significant cellular proliferation. Cardiomyocyte hypertrophy was assessed at the cellular level by measurement of cardiomyocyte cross-sectional area in hematoxylin and eosin–stained transverse LV sections from WT and Akt1-deficient mice after rest or after exercise training (Figure 2B). Cardiomyocyte cross-sectional area was significantly increased in WT mice after swimming training compared with sedentary WT mice (Figure 2C). Cardiomy-

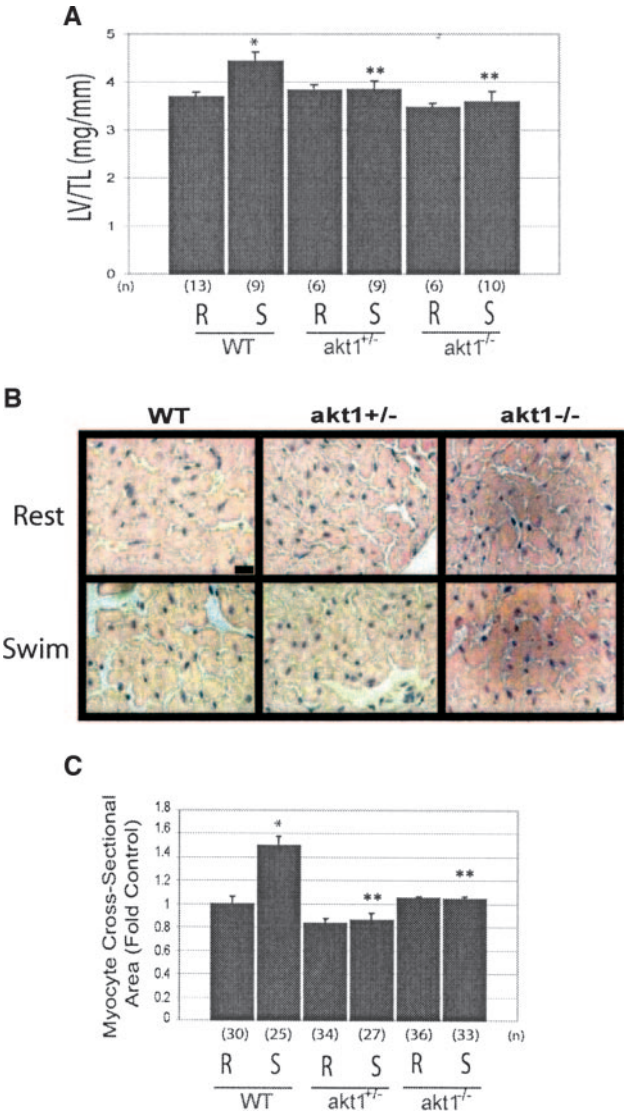

Figure 2. Akt1 is required for exercise-induced cardiac hypertrophy. A, Morphometric analysis of WT, akt1$^{+/-}$, and akt1$^{-/-}$ mice after 20 days rest (R) or swimming training (S). LV/TL was determined by morphometry. Number of animals analyzed in each group (n) is indicated in parentheses. To evaluate whether swimming training differentially affected WT, akt1$^{+/-}$, or akt1$^{-/-}$ mouse LV/TL, the following 2-tailed, 2-sample homoscedastic t tests were performed with Bonferroni's post hoc correction: WT resting vs WT swimming, akt1$^{+/-}$ swimming vs WT swimming, and akt1$^{-/-}$ swimming vs WT swimming. *P<0.05 vs resting WT mice; **P<0.05 vs WT swimming group. B, Histological analysis of cardiomyocyte cross-sectional area of WT, akt1$^{+/-}$, and akt1$^{-/-}$ mice after rest (R) or swimming training (S) for 20 days: low-power photomicrographic images of cardiac tissue sections stained with hematoxylin and eosin. Scale bar=20 μm. C, Average myocyte cross-sectional areas from transverse cardiac sections from WT, akt1$^{+/-}$, and akt1$^{-/-}$ mice subjected to 20 days of rest or swim training were determined by computerized photomicrographic analysis. Numbers of cells (n) measured in random fields in at least 3 mice per treatment group are shown in parentheses. To evaluate whether swimming training differentially affected WT, akt1$^{+/-}$, or akt1$^{-/-}$ mouse cardiomyocyte cross-sectional area, statistical comparisons were performed with Bonferroni's post hoc correction: WT resting vs WT swimming and akt1$^{-/-}$ swimming vs WT swimming (Mann Whitney), and akt1$^{+/-}$ swimming vs WT swimming (2-sample homoscedastic t test). *P<0.05 vs resting WT mice; **P<0.05 vs WT swimming group.

ocyte cross-sectional area was significantly lower in both akt1$^{+/-}$ and akt1$^{-/-}$ mice after swimming training compared with sedentary congenic mice (Figure 2C).

Normal G Protein–Coupled Receptor-Mediated Akt Pathway Signaling in Endothelin 1–Stimulated akt1$^{-/-}$ AMCMs

Recent evidence indicates that the adaptive, physiological cardiac growth profile is mediated by signaling pathways distinct from those that mediate pathological or maladaptive cardiac growth. Whereas physiological hypertrophy develops in response to stimuli such as IGF-1 stimulation or exercise training, pressure overload and chronic G protein–coupled receptor agonism are known to stimulate cardiac growth associated with interstitial fibrosis, abnormal gene expression, and progression to heart failure. The role of Akt1 in G protein–coupled receptor–mediated cardiac signal transduction was first probed in akt1$^{-/-}$ AMCMs stimulated with or without the GPCR ligand endothelin 1 (ET1; 200 mol/L). Surprisingly, ET1-stimulated Akt pathway signal transduction was indistinguishable in WT and Akt1-deficient AMCMs (Figure 3A). Indeed, the steady-state phosphorylation of downstream Akt targets GSK3B(S9), p70 S6 kinase (T389), and the S6 ribosomal subunit (S235/236) was unaltered in the presence or absence of Akt1.

Enhanced Protein Synthesis in Response to ET1 Treatment in akt1$^{-/-}$ AMCMs

We examined whether Akt1 was required for ET1-induced protein synthesis by measuring trichloroacetic acid–precipitable counts after a 24-hour pulse period with [^{3}H]-leucine (Figure 3B). WT cardiomyocytes incorporated more [^{3}H]-leucine in response to ET1 compared with WT vehicle-treated controls (15.7±2.6%), although this trend did not reach statistical significance. In striking contrast, ET1-treated akt1$^{-/-}$ cardiomyocytes exhibited an enhanced leucine incorporation response compared with vehicle-treated congenic controls (40.4±15.3% versus vehicle-treated akt1$^{-/-}$ cultures). The observed stimulation in protein synthesis was significantly greater than that observed in ET1-treated WT cardiomyocytes ($P<0.05$). The enhanced AMCM growth response to ET1 was corrected by acute wild-type Akt1 reconstitution by adenoviral transduction (Data Supplement Figure III).

Enhanced Cardiac Growth Response to Pressure Overload in akt1$^{-/-}$ Mice

To determine the role of Akt1 in pathological cardiac hypertrophy in response to pressure overload, TAC was performed on 8- to 12-week old akt1$^{+/-}$, akt1$^{-/-}$ mice, and their WT littermates. A survival rate of 100% in all genotypes was observed 1 week after TAC, and no differences in cardiomyocyte apoptosis were apparent across genotypes, as assessed by TUNEL and cleaved caspase-3 immunohistochemical analysis (not shown) of LV transverse sections. Echocardiographic analysis of LVMI confirmed that both akt1$^{+/-}$ and WT mice developed LV hypertrophy to a similar extent 7 days after TAC. In contrast, akt1$^{-/-}$ mice developed a trend toward more profound cardiac hypertrophy after TAC

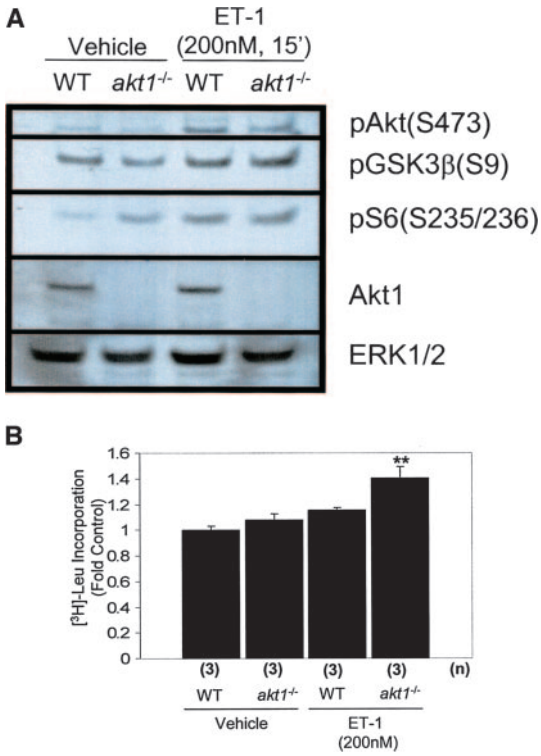

Figure 3. Enhanced hypertrophic response to ET1 in adult akt1$^{-/-}$ AMCMs. A, AMCM lysates from WT and akt1$^{-/-}$ mice stimulated with or without 200 nmol/L ET1 were subjected to phosphospecific Akt(S473), GSK3β(S9), and S6 (S235/236) ribosomal subunit immunoblotting. Blots were stripped and reprobed for ERK1/2 to control for loading. Akt1 immunoblots on stripped membranes confirmed the absence of Akt1 protein in akt1$^{-/-}$ mice. B, Incorporation of radiolabeled leucine was measured in WT and akt1$^{-/-}$ AMCMs stimulated with or without ET1 (200 nmol/L) for 24 hours in the presence of [^{3}H]-leucine. Data are expressed as mean [^{3}H]-leucine incorporation/μg protein±SD. This experiment was performed a minimum of twice with similar results in each experiment. Data shown are representative of 2 experiments, each performed in triplicate under each condition. One-way ANOVA with Tukey's post hoc correction was performed to simultaneously compare WT unstimulated, akt1$^{-/-}$ unstimulated, WT stimulated, akt1$^{-/-}$ unstimulated, and akt1$^{-/-}$ stimulated. **$P<0.05$ vs ET1-treated WT AMCMs.

that did not reach statistical significance compared with WT littermate controls (Table 3). The mean±SE LVMI determined by echocardiography was 5.55±0.66 mg/g in akt1$^{-/-}$ mice 7 days after TAC versus 3.95±0.23 and 3.96±0.24 mg/g in WT and heterozygous littermates, respectively. The Doppler flow gradient achieved by TAC was nearly identical for all 3 genotypes; therefore, the enhanced hypertrophic response observed in akt1$^{-/-}$ mice was not due to more stringent constriction of the transverse aorta. In addition to profound cardiac hypertrophy, akt1$^{-/-}$ mice developed cardiac dysfunction in response to TAC. Echocardiography of akt1$^{-/-}$ mice 7 days after TAC revealed LV dilatation and systolic dysfunction (Table 3). Mean LVIDs after TAC in akt1$^{-/-}$ mice was 2.30±0.24 versus 1.52±0.10 mm in TAC-operated WT mice ($P=0.033$). Mean FS was 54.9±2.4% in TAC-operated WT mice versus 36.3±4.2% in TAC-operated akt1$^{-/-}$ mice ($P=0.003$).

TABLE 3. Echocardiographic Analysis of Mice After TAC or Sham Operation

	Sham Operation			TAC Operation		
	WT (n=10)	akt1$^{+/-}$ (n=3)	akt1$^{-/-}$ (n=3)	WT (n=10)	akt1$^{+/-}$ (n=9)	akt1$^{-/-}$ (n=6)
Heart rate, min^{-1}	705±11	717±11	698±9.1	670±18	704±7.2	669±31
LVPWd, mm	0.65±0.01	0.73±0.03	0.58±0.05	0.72±0.03	0.74±0.03	0.78±0.09
IVSd, mm	0.70±0.02	0.73±0.06	0.61±0.04	0.79±0.04	0.81±0.02	0.82±0.09
LVIDd, mm	3.48±0.05	3.44±0.08	3.45±0.12	3.34±0.05	3.36±0.08	3.57±0.18
LVMI, mg/g	3.16±0.10	3.39±0.52	3.11±0.43	3.95±0.23*	3.96±0.24	5.55±0.66
LVIDs, mm	1.57±0.06	1.78±0.12	1.46±0.01	1.52±0.10	1.79±0.14	2.30±0.24†
FS, %	55.1±1.2	48.2±2.8	57.8±1.1	54.9±2.4	47.2±2.8	36.3±4.2†
Doppler velocity, m/s	...	...	...	4.13±0.16	4.40±0.21	4.30±0.12

Abbreviations as in Table 1. Eight- to twelve-week-old mice underwent transthoracic echocardiography 7 days after TAC or sham operation. Doppler velocity was measured at the site of TAC. To evaluate differences in the magnitude of TAC effects on cardiac parameters, the following statistical comparisons were performed with Bonferroni's post-hoc correction: WT sham vs WT TAC, akt1$^{+/-}$ TAC vs WT TAC, akt1$^{-/-}$ TAC vs WT TAC. Values are mean±SE.
*$P<0.05$ vs WT mice after sham operation; †$P<0.05$ vs WT after TAC operation.

The mean±SE LV/BW in WT animals increased from 3.40±0.03 mg/g after a sham operation to 4.21±0.13 mg/g after TAC. This represents a 23.8% increase relative to sham-operated WT mice. The cardiac hypertrophic response of akt1$^{+/-}$ mice to pressure overload was indistinguishable from that in WT mice (Figure 4A). akt1$^{-/-}$ mice, however, developed more profound hypertrophy after TAC compared with TAC-operated WT mice. The LV/BW in TAC-operated akt1$^{-/-}$ mice was 5.30±0.367 mg/g, which represents a 51% increase in LV/BW compared with sham-operated akt1$^{-/-}$ mice. The LV/BW in akt1$^{-/-}$ mice was significantly greater than the LV/BW in TAC-operated WT littermate controls ($P=0.015$ versus TAC-operated WT mice). Measurement and comparison of LV/TL across treatment groups yielded identical relationships (not shown). Cardiomyocyte cross-sectional area increased as a result of TAC for all 3 genotypes (Figure 4B), but the mean cross-sectional area was 41% greater in TAC-operated akt1$^{-/-}$ mice compared with TAC-operated WT mice ($P<0.001$; Figure 4C).

Gene expression analysis of cardiac tissue was evaluated by real-time quantitative RT-PCR after sham and after TAC operations. Mean ANF mRNA abundance increased in WT animals in response to TAC (Figure 4D, left). TAC-operated akt1$^{-/-}$ mice, however, exhibited ANF mRNA abundance that was significantly greater than that observed in TAC-operated WT mice.

β-myosin heavy chain (βMHC) mRNA abundance increased in WT animals in response to TAC (Figure 4D). In akt1$^{-/-}$ mice, cardiac βMHC mRNA at baseline was elevated relative to WT mice at baseline. βMHC mRNA abundance was also greater in akt1$^{+/-}$ mice and in akt1$^{-/-}$ after TAC compared with TAC-operated WT mice. Histological analysis of LV sections stained with Masson's trichrome revealed no detectable difference in the ability of Akt1-deficient mice to develop cardiac interstitial fibrosis either before or after TAC compared with WT mice (not shown).

Discussion

In this work, we analyzed the role of Akt1 in cardiac growth in response to various physiological and pathological stimuli. Previous work demonstrated that the cardiac responses elicited by pressure overload or ET1 stimulation differ greatly from those stimulated by exercise training or IGF-1 infusion. Pressure overload promotes a deleterious form of cardiac hypertrophy characterized by cardiac fibrosis and dysfunction, whereas exercise training and IGF-1 promote a physiological form of cardiac hypertrophy characterized by improved cardiac function without cardiac fibrosis or fetal gene induction.[26] Here, we demonstrate that Akt1 is absolutely required for physiological growth in response to IGF-1 stimulation or to exercise training, whereas Akt1 negatively regulates ET1- and TAC-induced cardiac hypertrophy.

The present study also demonstrates that the absence of Akt1 profoundly exacerbates the TAC-stimulated cardiac hypertrophic program, although the model used in these studies is not without limitations. That developmental, systemic, or other compensatory differences might contribute to the phenotypes observed in the present study remains a possibility. However, transient adenoviral reconstitution of WT Akt1 in cultured adult akt1$^{-/-}$ mouse cardiomyocytes rescued the exacerbated ET1-stimulated cardiomyocyte hypertrophic response as measured by radiolabeled [^{3}H]-leucine incorporation (Data Supplement Figure III). Additionally, the steady-state levels of potentially compensatory kinases (eg, Akt2, ILK, PI3Kα) were indistinguishable from those in WT mice.

The mechanism that explains the negative regulation of pathological hypertrophy by Akt1 remains unclear, although cross-talk through several candidate pathways remains under investigation. Previous studies demonstrate inhibitory effects of Akt signaling on the ERK and JNK MAP kinase pathways,[27,28] both of which enhance growth in the myocardium.[23,24,29] Thus, hyperactivation of the MAPKs in an Akt1-deficient model might explain the present observations. Equally promising in the akt1$^{-/-}$ model will be the investigation of calcineurin/NFAT pathway activation, which itself is a critical mediator of pathological, but not physiological, cardiac hypertrophy.[30] Moreover, the residual Akt phosphorylation in akt1$^{-/-}$ AMCMs in response to ET1 stimulation

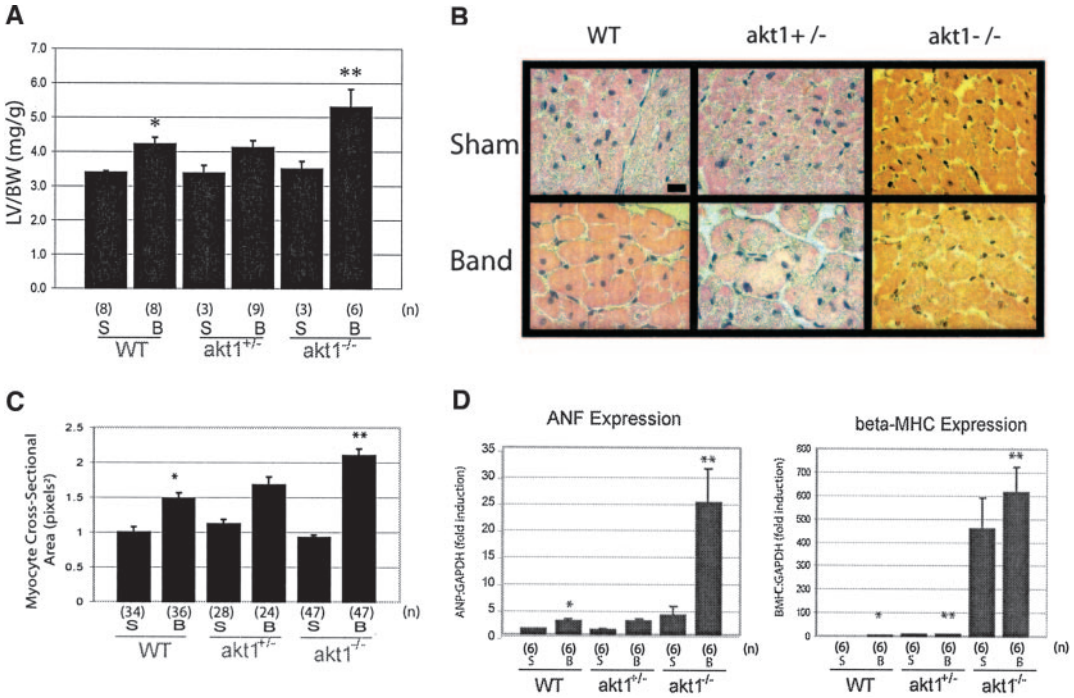

Figure 4. Akt1 antagonizes the hypertrophic response to pressure overload. A, LV/BW determined by morphometry in akt1$^{-/-}$, akt1$^{+/-}$, and WT mice 7 days after sham (S) or TAC (B) operation. To determine whether the magnitude of response to TAC was differentially affected in WT, akt1$^{+/-}$, and akt1$^{-/-}$ mice, the following statistical comparisons were performed with Bonferroni's post hoc correction: WT sham vs WT band and akt1$^{+/-}$ band vs WT band (2-sample, 2-tailed homoscedastic *t* tests), and akt1$^{-/-}$ band vs WT band (Mann-Whitney). *P<0.05 vs sham-operated WT mice; **P<0.05 vs WT band. For each group, values in parentheses (n) indicate the number of animals analyzed in each group. B, Histological analysis of cardiomyocyte cross-sectional area 7 days after TAC. Displayed are low-power photomicrographs of transverse cardiac sections stained with hematoxylin and eosin. Scale bar=20 μm. C, Cardiomyocyte cross-sectional area determined by computerized analysis of transverse cardiac section photomicrographs. Mean fold change in cross-sectional area±SE is shown. The sample size in each group (n) is indicated in parentheses. *P<0.05 vs sham-operated WT mice; **P<0.05 vs TAC-operated WT mice. D, Akt1 antagonizes TAC-induced ANP and β-MHC expression. Cardiac ANP (left) and β-MHC (right) gene expression normalized by GAPDH expression was determined by real-time quantitative RT-PCR 7 days after TAC (B) or sham (S) operation in akt1$^{-/-}$, akt1$^{+/-}$, and WT mice. Shown is the mean fold change in normalized gene expression±SE. The number of samples analyzed (n) in each group is shown in parentheses. To determine whether the magnitude of ANP response to TAC was differentially affected in WT, akt1$^{+/-}$, and akt1$^{-/-}$ mice, the following statistical comparisons were performed: akt1$^{+/-}$ TAC vs WT TAC and akt1$^{-/-}$ TAC vs WT TAC (Mann-Whitney test), and WT sham vs WT TAC (2-tailed homoscedastic *t* test). β-MHC expression was analyzed by the Mann-Whitney test in WT sham vs WT TAC and in WT TAC vs akt1$^{-/-}$ TAC. WT TAC vs akt1$^{+/-}$ β-MHC levels were compared by 2-tailed homoscedastic *t* test. Bonferroni post hoc correction was applied in all cases. *P<0.05 vs sham-operated WT mice; **P<0.05 vs WT band.

(Figure 3A) precludes us from ruling out Akt2 as a mediator of pathological cardiac growth.

Sustained GSK3β(ser9) phosphorylation in response to ET1 stimulation in akt1$^{-/-}$ AMCMs permits additional speculation that the antihypertrophic effects mediated by GSK3β are inactive in the akt1$^{-/-}$ heart after provocative stimuli. This lack of antihypertrophic signaling may hypersensitize the akt1$^{-/-}$ heart to growth-promoting signal transduction (eg, via the MAPK or calcineurin signaling pathways). Furthermore, the profound hypertrophy observed in response to TAC even in the presence of elevated ANP gene activation suggests that the antihypertrophic and cardioprotective effects of ANF in the myocardium[31,32] either are disrupted or are insufficient in the absence of Akt1. The use of compound genetic murine models to understand the growth-promoting signaling pathways regulated by Akt1 will be imperative in defining candidate pharmacotherapeutic targets for the treatment of pathological cardiac hypertrophy and progression to heart failure.

In conclusion, our studies elucidate for the first time a dual adaptive function of Akt1 to suppress pathological cardiac hypertrophy and promote physiological hypertrophy. Agents that increase Akt1 activity in heart tissue such as IGF-1 are likely to promote the development of adaptive cardiac growth and may therefore be of therapeutic utility.

Acknowledgments

This work was supported by grants from the NIH (HL-61567, HL-057278) and the Burroughs Wellcome Fund (A.J.M.). B.J. DeBosch was supported by the Cardiovascular Physiology Training grant T32-HL07873. The akt1$^{-/-}$ mice used throughout these studies were a kind gift from Morris Birnbaum, Howard Hughes Medical Institute, University of Pennsylvania School of Medicine. We acknowledge the assistance of the Washington University Digestive Diseases Research Core Center (NIH P30 DK52574) and of Dr William Shannon, Director, Washington University School of Medicine Biostatistical Consulting Center.

Disclosures

None.

References

1. Sadoshima J, Izumo S. The cellular and molecular response of cardiomyocytes to mechanical stress. *Annu Rev Physiol*. 1997;59:551–571.

2. Levy D, Garrison RJ, Savage DD, Kannel WB, Castelli WP. Prognostic implications of echocardiographically determined left ventricular mass in the Framingham Heart Study. *N Engl J Med*. 1990;322:1561–1566.
3. Messerli FH, Soria F. Hypertension, left ventricular hypertrophy, ventricular ectopy, and sudden death. *Am J Med*. 1992;93:21S–26S.
4. Longhurst JC, Stebbins CL. The power athlete. *Cardiol Clin*. 1997;15:413–429.
5. Shepard RJ. The athlete's heart: is big beautiful? *Br J Sports Med*. 1996;30:5–10.
6. Cho KS, Lee JH, Kim S, Kim D, Koh H, Lee J, Kim C, Kim J, Chung J. *Drosophila phosphoinositide*–dependent kinase-1 regulates apoptosis and growth via the phosphoinositide-3-kinase–dependent signaling pathway. *Proc Natl Acad Sci U S A*. 2001;98:6144–6149.
7. Lawlor MA, Alessi DR. PKB/Akt: a key mediator of cell proliferation, survival and insulin responses. *J Cell Sci*. 2001;114:2903–2910.
8. Mende I, Malstrom S, Tsichlis PN, Vogt PK, Aoki M. Oncogenic transformation induced by membrane-targeted Akt2 and Akt3. *Oncogene*. 2001;20:4419–4423.
9. Potter CJ, Pedraza LG, Zu T. Akt regulates growth by directly phosphorylating Tsc2. *Nat Cell Biol*. 2002;4:658–665.
10. Inoki K, Li Y, Zhu T, Wu J, Guan KL. TSC2 is phosphorylated and inhibited by Akt and suppresses mTOR signaling. *Nat Cell Biol*. 2002;4:648–657.
11. Faridi J, Fawcett J, Wang L, Roth RA. Akt promotes increased mammalian cell size by stimulating protein synthesis and inhibiting protein degradation. *Am J Physiol Endocrinol Metab*. 2003;285:E964–E972.
12. Datta SR, Brunet A, Greenberg ME. Cellular survival: a play in three Akts. *Genes Dev*. 1999;13:2905–2927.
13. van Weeren PC, de Bruyn KM, de Vries-Smits AM, van Lint J, Burgering BM. Essential role for protein kinase B (PKB) in insulin-induced glycogen synthase kinase 3 inactivation: characterization of dominant-negative mutant of PKB. *J Biol Chem*. 1998;273:13150–13156.
14. Oh H, Fujio Y, Kunisada K, Hirota H, Matsui H, Kishimot T, Yamauchi-Takihara K. Activation of phosphatidylinositol 3-kinase through glycoprotein induces protein kinase B and p70 S6 kinase phosphorylation in cardiomyocytes. *J Biol Chem*. 1998;273:9703–9710.
15. Schluter KD, Goldberg Y, Taimor G, Schafer M, Piper HM. Role of phosphatidylinositol 3-kinase activation in the hypertrophic growth of adult ventricular cardiomyocytes. *Cardiovasc Res*. 1998;40:174–181.
16. Shioi T, Kang PM, Douglas PS, Hampe J, Yballe CM, Lawitts J, Cantley LC, Izumo S. The conserved phosphoinositide 3-kinase pathway determines heart size in mice. *EMBO J*. 2000;19:2537–2548.
17. McMullen JR, Shioi T, Zhang L, Tarnavski O, Sherwood MC, Kang PM, Izumo S. Phosphoinositide 3-kinase (p110alpha) plays a critical role for the induction of physiological, but not pathological, cardiac hypertrophy. *Proc Natl Acad Sci U S A*. 2003;100:12355–12360.
18. Shioi T, McMullen JR, Kang PM, Douglas PS, Obata T, Franke TF, Cantley LC, Izumo S. Akt/protein kinase B promotes organ growth in transgenic mice. *Mol Cell Biol*. 2002;22:2799–2809.
19. Matsui T, Li L, Wu JC, Cook SA, Nagoshi T, Picard MH, Liao R, Rosenzweig A. Phenotypic spectrum caused by transgenic overexpression of activated Akt in the heart. *J Biol Chem*. 2002;277:22896–22901.
20. Cho H, Mu J, Kim JK, Thorvaldsen JL, Chu Q, Crensha EB, Kaestner KH, Bartolomei MS, Shulman GI, Birnbaum MJ. Insulin resistance and a diabetes mellitus–like syndrome in mice lacking the protein kinase Akt2 (PKB beta). *Science*. 2001;292:1728–1731.
21. Cho H, Thorvaldsen JL, Chu Q, Feng F, Birnbaum MJ. Akt1/PKBalpha is required for normal growth but dispensable for maintenance of glucose homeostasis in mice. *J Biol Chem*. 2001;276:38349–38352.
22. Sambrano GR, Frase I, Han H, Ni Y, O'Connel T, Yan Z, Stull JT. Navigating the signaling network in mouse cardiac myocytes. *Nature*. 2002;420:712–714.
23. Harris IS, Zhang S, Treskov I, Kovacs A, Weinheimer C, Muslin AJ. Raf-1 kinase is required for cardiac hypertrophy and cardiomyocyte survival in response to pressure overload. *Circulation*. 2004;110:718–723.
24. Xing H, Zhang S, Weinheimer C, Kovacs A, Muslin AJ. 14–3–3 Proteins block apoptosis and differentially regulate MAPK cascades. *EMBO J*. 2000;19:349–358.
25. Scheinowitz M, Kessler-Icekson G, Freimann S, Zimmermann R, Schaper W, Golomb E, Savion N, Eldar M. Short- and long-term swimming exercise training increases myocardial insulin-like growth factor-I gene expression. *Growth Horm IGF Res*. 2003;13:19–25.
26. Tanaka N, Ryoke T, Hongo M, Mao L, Rockman HA, Clark RG, Ross J. Effects of growth hormone and IGF-1 on cardiac hypertrophy and gene expression in mice. *Am J Physiol*. 1998;275:H393–H399.
27. Zimmermann S, Moelling K. Phosphorylation and regulation of raf by Akt (protein kinase B). *Science*. 1999;286:1741–1744.
28. Kim AH, Sasaki T, Chao MV. Akt1 regulates a JNK scaffold during excitotoxic apoptosis. *Neuron*. 2002;35:697–709.
29. Choukroun G, Hajjar R, Fry S, del Monte F, Haq S, Guerrero JL, Picard M, Rosenzweig A, Force T. Regulation of cardiac hypertrophy in vivo by the stress-activated protein kinases/c-Jun NH(2)-terminal kinases. *J Clin Invest*. 1999;104:391–398.
30. Wilkins BJ, Dai YS, Bueno OF, Parsons SA, Xu J, Plank DM, Jones F, Kimball TR, Molkentin JD. Calcineurin/NFAT coupling participates in pathological, but not physiological, cardiac hypertrophy. *Circ Res*. 2004;94:110–118.
31. Kato T, Muraski J, Chen Y, Tsujita Y, Wall J, Glembotski CC, Schaefere E, Beckerle M, Sussman MA. Atrial natriuretic peptide promotes cardiomyocyte survival by cGMP-dependent nuclear accumulation of zyxin and Akt. *J Clin Invest*. 2005;115:2716–2730.
32. Rosenkranz AC, Woods RL, Dusting GJ, Ritchie RH. Antihypertrophic actions of the natriuretic peptides in adult rat cardiomyocytes: importance of cyclic GMP. *Cardiovasc Res*. 2003;57:515–522.

CLINICAL PERSPECTIVE

Hypertension and aortic stenosis lead to the development of a pathological form of cardiac hypertrophy that contributes to the development of congestive heart failure and cardiac arrhythmias. On the other hand, elite athletes often develop a physiological form of cardiac hypertrophy that is associated with a favorable prognosis and is not associated with cardiac arrhythmias or the development of congestive heart failure. In this work, mice lacking an intracellular protein kinase, Akt1, were resistant to the development of physiological cardiac hypertrophy in response to swimming exercise, but were sensitized to the development of pathological hypertrophy after constriction of the transverse aorta, a model of hypertension. These results suggest that agents that increase Akt1 activity or expression might promote physiological growth of the heart while antagonizing pathological growth and may therefore have therapeutic utility in the treatment of hypertensive heart disease and congestive heart failure. One hope is that it will be possible to convert pathological cardiac hypertrophy to a more adaptive, physiological form. Several growth factors and hormones are known to activate Akt1 in heart tissue, including growth hormone, insulin-like growth factor-1, fibroblast growth factor, and epidermal growth factor.

Akt1 Is Required for Physiological Cardiac Growth

Brian DeBosch, Iya Treskov, Traian S. Lupu, Carla Weinheimer, Attila Kovacs, Michael Courtois and Anthony J. Muslin

Circulation. 2006;113:2097-2104; originally published online April 24, 2006;
doi: 10.1161/CIRCULATIONAHA.105.595231
Circulation is published by the American Heart Association, 7272 Greenville Avenue, Dallas, TX 75231

Print ISSN: 0009-7322. Online ISSN: 1524-4539